Detector Noise Model Verification For Undersea Free Space Optical Data Links

David Rashkin, Ionut Cardei, Mihaela Cardei
Department of Computer & Electrical Engineering and Computer Science
Florida Atlantic University
Boca Raton, FL, USA

Fraser Dalgleish
Ocean Visibility and Optics Lab
Harbor Branch Oceanographic Institute
Fort Pierce, FL, USA

Thomas Giddings
Metron, Inc.
Reston, VA, USA

I. Introduction

The need for midrange, high throughput data networks in the undersea environment is evident for a variety of applications, including sensor networks and remote control and telemetry for unmanned underwater vehicles. While research continues into undersea acoustic and radio frequency networks, results show that these suffer from low data rates (in the case of the former) or severe range limitations (in the case of the latter) [1]. Free space optical technology provides a good balance between data throughput and potential distance between communicating nodes; given the cost of deploying and testing these types of networks, however, it is necessary to develop accurate models that allow us to simulate digital communication between nodes, facilitating the development of optimal protocols at low cost. One important component of such a system is an accurate model for the noise in the detector output signal. This paper evaluates one such model [2] for its suitability in predicting shot noise (the random variation in the detector output signal that is caused by the random arrival times of the photons at the detector photocathode) and the noise introduced by a Photomultiplier Tube (PMT) detector.

We analyze the noise in a new high-efficiency PMT, and compare the experimental signal-to-noise ratio (SNR) with the SNR obtained using two different theoretical models. The first model, referred to in this paper as the standard model, arrives at an average SNR value for a particular input signal by using Poisson counting statistics, which is generally accepted as a predictor for shot-noise-limited devices such as PMTs [3][4]. The alternative approach models the detector output signal as a compound Poisson stochastic process, which adds noise to a clean signal on a per-sample basis. This is much more useful than an average predicted SNR, as it allows us to simulate the actual bit error rate (BER), based on received samples, and obtain a simulation framework for predicting BER as a function of SNR (and thus to predict BERs for various scenarios involving different geometric and environmental parameters).

Our setup uses a continuous wave laser operating at a wavelength of λ=532 nm. The photon flux entering the PMT is varied using neutral density filters, while the gain voltage is varied to obtain several sets of data captured by an analog-to-digital converter (ADC). This data was then analyzed to produce experimental SNR measurements. For each of the experimental SNR measurements, we then calculated the predicted SNR using both the standard model and the stochastic process model, and compare both against the experimental SNR measurements.

We show that the stochastic process noise model is more accurate in predicting average SNR at low-power conditions than the accepted standard model for average SNR of a shot-noise-limited PMT. By validating the average SNR predictions of the stochastic model vs the standard model, we conclude that the stochastic model is appropriate for use in simulating the noise in a signal produced by a PMT. This ultimately will allow us to build accurate physical layer simulations of free-space optical undersea communication networks, which in turn will allow us to simulate and optimize the higher layer protocols in the network stack.

We continue this paper in Section II with an introduction to the standard average SNR model and in Section III with a discussion of the novel compound stochastic noise model. In Section IV we discuss the laboratory setup for the experimental validation and in Section V we discuss the numeric results. We conclude this paper and discuss future directions for research in Section VI.

II. Standard Textbook Noise model

The standard model for predicting the average SNR of a photon detector is defined as [4]:

$$SNR = \frac{(G\eta F q P/hf)^2 R_L}{G^2 2 q R_L \Delta f (I_D + \eta F q P/hf) + 4kT\Delta f} \quad (1)$$

Where G is the applied detector gain, η is the quantum efficiency of the photocathode, F is the collection efficiency of the detector (ηF is the overall detector efficiency), q is the elementary charge, P is the optical power incident on the photocathode, h is Planck's constant, f is the frequency of the light, R_L is the resistance over which a voltage signal is measured, Δf is the detector bandwidth, I_D is the dark current, k is the Boltzmann constant, and T is the temperature.

For so-called shot-noise-limited photon detectors, such as PMTs, the shot noise is significantly larger than both the dark current and the thermal noise, so these other noise sources are

ignored, and the SNR is typically defined in terms of the root-mean-squared (rms) shot-noise current that manifests as a result of a dc current flow, $i_{avg,}$ as given in [3]:

$$\sigma_i = \sqrt{2q\, i_{avg}\, \Delta f} \tag{2}$$

and the SNR is given by:

$$SNR_{signal-shot-limit} = \frac{i_{avg}}{i_{noise,rms}} = \frac{i_{avg}}{\sqrt{2q\, i_{avg}\, \Delta f}} \tag{3}$$

III. Compound Poisson Stochastic Process Model

Shot noise is the random variation in the detector output signal that is caused by the random arrival times of the photons at the detector photocathode. As such, the electrical signal output from the detector can be regarded as a continuous random function driven by a discrete Poisson counting process. Below we outline the derivation of the mean, variance, and autocovariance of the stochastic shot noise process. The derivation is similar to the presentations in van Etten [5] and Ross [6], and is fully documented in reference [2].

The photomultiplier output $X(t)$ is modeled as a non-stationary compound Poisson process,

$$X(t) = \sum_{k=1}^{N(t)} G_k \mathrm{h}(t - S_k) \tag{4}$$

where $N(t)$ is the number of photons striking the photocathode up to time t, S_k is the arrival time of the k^{th} photon, G_k is the random amplifier gain, and h is the electrical impulse response of the detector. The average photon arrival rate $\gamma(t)$ is time-dependent, and we define

$$\upsilon(t) = E[N(t)] = \int_0^t \gamma(s) ds. \tag{5}$$

where $E[\,]$ denotes the expectation. The arrival time distribution is (for $n \geq 0$)

$$\begin{aligned} &P\{N(s+t) - N(s) = n\} \\ &= \exp\left(-[\upsilon(t+s) - \upsilon(s)]\right) \frac{[\upsilon(t+s) - \upsilon(s)]^n}{n!}, \end{aligned} \tag{6}$$

so that the increments are independent. Note that $P\{N(t) = n\} = \exp(-\upsilon(t))(\upsilon(t))^n / n!$. The arrival times over the interval $s \in [0, t]$ are distributed according to the probability density function (see [7] and references therein)

$$f_{S_k}(s) = \frac{\gamma(s)}{\upsilon(t)}, \tag{7}$$

which is independent of the number of arrivals $N(t)$ over the interval.

The detector impulse response, h for $t \geq 0$, is assumed to be deterministic and stationary so that the pulse shape is always the same. The autocorrelation of the impulse response is denoted by

$$C_{\mathrm{h}}(\tau) = \int_{-\infty}^{+\infty} \mathrm{h}(t - \tau)\, \mathrm{h}(t)\, d\tau. \tag{8}$$

We consider a detector with random fluctuations in amplification so that $\{G_k\}$ is a sequence of independent, identically distributed random variables. The moment generating function for G is

$$\Phi_G(y) = E[\exp(yG)], \tag{9}$$

where the mean, or expectation, is $\mu_G = \Phi_G'(0)$ and variance is $\sigma_G^2 = \Phi_G''(0) - \mu_G^2$.

The moment generating function for the shot noise process can be derived using the conditional expectation and invoking the independence of the random variables,

$$\begin{aligned} \Phi_X(u) &= E[\exp(uX)] \\ &= \exp\left\{\int_0^t \gamma(s)\left[\Phi_G(u\, \mathrm{h}(t-s)) - 1\right] ds\right\} \end{aligned} \tag{10}$$

From this we can calculate the mean and variance of the shot noise process,

$$\mu_X(t) = \Phi_X'(0) = E[G] \int_0^t \gamma(s)\, \mathrm{h}(t-s)\, ds \tag{11}$$

$$\sigma_X^2(t) = \Phi_X''(0) - \mu_X^2 = E[G^2] \int_0^t \gamma(s)\, \mathrm{h}^2(t-s)\, ds \tag{12}$$

where $E[G]$ and $E[G^2]$ are the first and second moments of the random detector gain. To derive the joint moment generating function for the shot noise process we consider

$$X_1(t) = \sum_{k=1}^{N(t_1)} G_k \mathrm{h}(t - S_k) \quad \text{for} \quad t \geq t_1 \tag{13}$$

and

$$X_2(t) = \sum_{k=1}^{N(t_2)} G_k\, \mathrm{h}(t - S_k) \quad \text{for} \quad t \geq t_2 \tag{14}$$

where $t_2 \geq t_1$. We can now write

$$X_2(t) = X_1(t) + \sum_{k=N(t_1)+1}^{N(t_2)} G_k\, \mathrm{h}(t - S_k) = X_1(t) + \bar{X}_2(t) \tag{15}$$

where X_1 and $\bar{X}_2$ are independent random variables [6]. The joint moment generating function is then

$$\begin{aligned} \Phi_{XX}(u_1, u_2) &= E\left[\exp\left\{u_1 X_1(t_1) + u_2 X_2(t_2)\right\}\right] \\ &= E\left[\exp\left\{u_1 X_1(t_1) + u_2 X_1(t_2)\right\}\right] E\left[\exp\left\{u_2 \bar{X}_2(t_2)\right\}\right]. \end{aligned} \tag{16}$$

The first term can be expressed as

$$\begin{aligned} &E\left[\exp\left\{u_1 X_1(t_1) + u_2 X_1(t_2)\right\}\right] \\ &= \exp\left\{\int_0^{t_1} \gamma(s)\left[\Phi_G\left(u_1 \mathrm{h}(t_1 - s) + u_2 \mathrm{h}(t_2 - s)\right) - 1\right] ds\right\}, \end{aligned} \tag{17}$$

and the second term is

$$E\left[\exp\left[u_2 \bar{X}_2(t_2)\right]\right] = \exp\left\{\int_{t_1}^{t_2} \gamma(s)\left[\Phi_G\left(u_2 \mathrm{h}(t_2-s)\right)-1\right]ds\right\}, \quad (18)$$

and finally we have

$$\Phi_{XX}(u_1, u_2) = \exp\left\{\int_0^{t_1} \gamma(s)\left[\Phi_G\left(u_1 \mathrm{h}(t_1-s)+u_2 \mathrm{h}(t_2-s)\right)-1\right]ds\right\} \times\exp\left\{\int_{t_1}^{t_2} \gamma(s)\left[\Phi_G\left(u_2 \mathrm{h}(t_2-s)\right)-1\right]ds\right\} \quad (19)$$

The autocovariance function is then given by

$$C_{XX}(t_1,t_2) = \left.\frac{\partial^2 \Phi_{XX}}{\partial u_1\, \partial u_2}\right|_{u_1, u_2=0} - \mu_X(t_1)\mu_X(t_2) = E[G^2]\int_0^{t_1} \gamma(s)\, \mathrm{h}(t_1-s)\, \mathrm{h}(t_2-s)\, ds \quad (20)$$

Higher-order statistics can also be derived from the moment generating function.

For the simulations we take G_k to be Gaussian distributed. The detector impulse response h is approximated with a Gaussian shape. If the mean radiant power incident on the detector surface is $P(t)$, the mean photon arrival rate is given by $\bar{\phi}(t)=P(t)/(\hbar\omega)$, where $h=6.63\times10^{-34}$ J·s is Planck's constant, $\hbar=h/2\pi$, the frequency of light for a wavelength of λ meters is $\nu=c/\lambda$ Hz, the angular frequency is $\omega=2\pi\nu$, and $c=3\times10^8$ m/s is the speed of light in a vacuum. The average rate of photon arrivals at the photocathode resulting in a pulse at the anode is then $\gamma(t)=\bar{\phi}(t)\eta F$.

For the detector output signal we consider samples $x_k=x(t_k)$ at times $t_k=k\Delta t$ for $k=0,1,2,\ldots$. We let $\boldsymbol{x}_n=(x_0, x_1, \ldots, x_n)^T$ be the vector of samples up to time t_n, where superscript 'T' indicates the transpose. The detector output signal $X(t_k)$ is modeled as a multivariate Gaussian distribution, which is easy to implement but results in some (non-physical) negative values for the output current. Noting that the correlation between nearby samples is much greater than that between more distant samples, we truncate the number of samples considered simultaneously in the joint density at some limit p.

The following outlines the procedure used to the simulate detector output signal. The joint probability density for signal samples is then

$$f_X(\boldsymbol{x}_n)=\frac{1}{(2\pi)^{n/2}|\Sigma|^{1/2}}\ \exp\left(-\frac{1}{2}(\boldsymbol{x}_n-\boldsymbol{\mu})^T\Sigma^{-1}(\boldsymbol{x}_n-\boldsymbol{\mu})\right) \quad (21)$$

where the vector of mean values is

$$\boldsymbol{\mu}_X=(\mu_{n-p},\ldots,\mu_n)^T=\mu_G(\gamma_{n-p},\ldots,\gamma_n)^T, \quad (22)$$

where $\mu_k=\mu_X(t_k)$ and $\gamma_k=\gamma(t_k)$, and the covariance matrix is

$$\Sigma = \begin{bmatrix} C_{n-p,n-p} & \cdots & C_{n-p,n} \\ \vdots & \ddots & \vdots \\ C_{n,n-p} & \cdots & C_{n,n} \end{bmatrix} \quad (23)$$

where $C_{j,k}=C_{XX}(t_j,t_k)$. We consider the vector of prior samples $\tilde{\boldsymbol{x}}=(x_{n-1},\ldots,x_{n-1})^T$ and define

$$\tilde{\boldsymbol{\mu}}=(\mu_{n-p},\ldots,\mu_{n-1})^T \quad \text{and} \quad \tilde{\boldsymbol{s}}=(C_{n-p,n},\ldots,C_{n-1,n})^T, \quad (24)$$

and

$$\tilde{\Sigma} = \begin{bmatrix} C_{n-p,n-p} & \cdots & C_{n-p,n-1} \\ \vdots & \ddots & \vdots \\ C_{n-1,n-p} & \cdots & C_{n-1,n-1} \end{bmatrix}. \quad (25)$$

The conditional density is then

$$f_X(x_n|\tilde{\boldsymbol{x}})=\frac{1}{\sqrt{2\pi}\bar{\sigma}_n}\ \exp\left(-\frac{1}{2}\frac{(x_n-\bar{\mu}_n)^2}{\bar{\sigma}_n^2}\right) \quad (26)$$

with

$$\bar{\mu}_n = \mu_n + \tilde{\boldsymbol{s}}^T\tilde{\boldsymbol{\Sigma}}^{-1}(\tilde{\boldsymbol{x}}-\tilde{\boldsymbol{\mu}}) \quad \text{and} \quad \bar{\sigma}_n^2 = \sigma_n^2-\tilde{\boldsymbol{s}}^T\tilde{\boldsymbol{\Sigma}}^{-1}\tilde{\boldsymbol{s}}. \quad (27)$$

Given the mean power incident on the receiver aperture at the discrete sample times we can use equation (26), together with the definitions in (27), to make consecutive random draws for the samples.

IV. Laboratory Test Setup

In our first set of experiments, we used a (Laser Quantum) Gem Laser source having a wavelength of 532 nm. We set the output power to a constant 86mW and used neutral density (ND) filters to control the photon flux entering the detector. The detector itself was a Hamamatsu R9880U-210 ultra bialkali photomultiplier tube. The detector output was measured using a National Instruments PXIe-6366 analog-to-digital converter (ADC), measuring the voltage across a $1k\,\Omega$ load. We also ran a second set of experiments using a slightly lower source output power of 50 mW.

V. Laboratory Test Results

To characterize the system noise floor, we covered the PMT input window with a screw-on cap to eliminate any light from entering the PMT. For each of the Gain Voltages used in the preceding experiments, we measured the detector output. The mean voltage measured by the ADC capture tool varied between -636.26 μV and -629.96 μV.

According to the PMT specifications, the Dark Current should be:

Gain Voltage	503V	598V	625V	639V	756V	839V	876V	1025V
Dark Current	0.004nA	0.015nA	0.017nA	0.02nA	0.08nA	0.2nA	0.3nA	1.25nA
Measured Voltage (V = IR) with R= 1000Ω	0.004μV	0.015μV	0.017μV	0.02μV	0.08μV	0.2μV	0.3μV	1.25μV

Note that, using a ±1.25 V scale, the NI PXIe-6366 has an absolute accuracy at full scale of around 300 μV according to the documentation. This implies that the ADC used is not nearly accurate enough to capture output resulting from Dark Current alone.

The presence of negative voltages in the noise floor is unexpected, since the PMT output should always result in positive measured voltage. We rule out possible sources of negative measured voltage:

- Johnson Noise

  $$V_{rms} = \sqrt{4 k_B T R \Delta f}$$

  where k_B is the Boltzmann constant, T is the temperature, R is the resistance across which the voltage is measured, and Δf approximately equal to the reciprocal of twice the sampling interval. For our $R = 1\text{k}\Omega$ resistor at room temperature and a 500 ns sampling interval, we get $V_{rms} = 4.0431$ μV. Note that the measured output mean is over 100 times greater than this value.
- Quantization Noise
  Total voltage range = 1.25 - (-1.25) = 2.5V
  Number of ADC bits = 16
  LSB corresponds to:

  $$LSB = \frac{2.5}{2^{16}} = 38.147\mu V$$

  In the rounding case, V_{rms} is given by:

  $$V_{rms} = \frac{1}{\sqrt{12}} LSB = 11.0121\mu V$$

  (with 0 mean)
  In the truncation case, V_{rms} is given by:

  $$V_{rms} = \frac{1}{\sqrt{3}} LSB = 22.0242\mu V$$

  with mean given by:

  $$\mu = \frac{1}{2} LSB = 19.0735\mu V$$

Given that neither Johnson noise nor quantization noise can account for the negative voltage recorded, we assume that the negative voltage is due to miscalibration of the ADC, and all subsequent calculations related to mean and standard deviation are modified by subtracting the noise floor mean and noise floor standard deviation:

$$\mu_{corrected} = \mu_{measured} - \mu_{noisefloor} \tag{28}$$

$$\sigma_{corrected} = \sqrt{\sigma^2_{measured} - \sigma^2_{noisefloor}} \tag{29}$$

Data was recorded in signed 16-bit integers, converted to volts (±1.25 V) according to:

$$V(t) = \frac{2.5\,(D(t) + 32768)}{65535} - 1.25 \tag{30}$$

$$I(t) = \frac{V(t)}{1000\,\Omega} \tag{31}$$

and converted to Amps by dividing by 1000 (documented resistance used) to obtain the output current measured by the detector. The following graphs were obtained for each experiment by taking the mean output current value for each gain voltage/neutral density filter (GV/ND) combination, and plotting against an 86 mW source signal, attenuated according to the documented ND filter values.

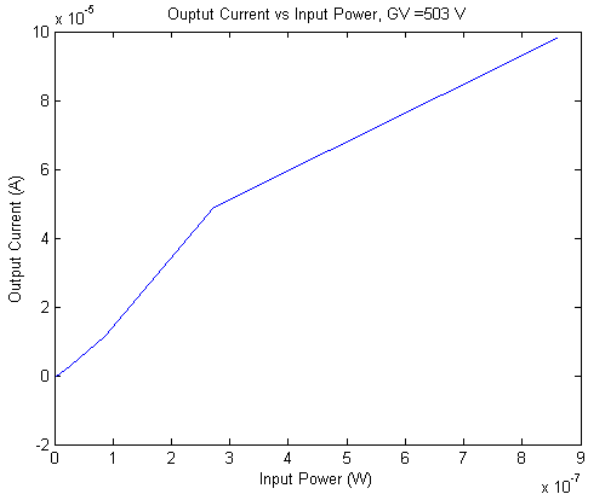

Figure 1: Detector response linearity.

The gain curves were then calculated by converting optical power to current,

$$I(t) = P(t)\,\frac{\lambda \eta}{\nu h e} \tag{32}$$

and comparing the output to the input

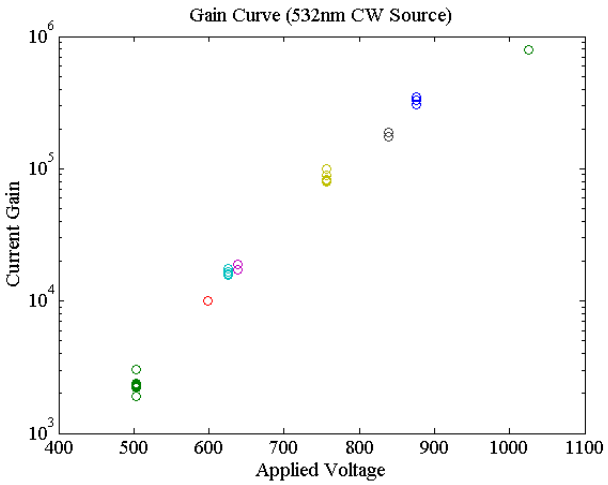

Figure 2: Current gain vs applied gain voltage.

In observing the raw captured data from the detector, we can see that for low ND filter values (higher number of photons striking the PMT) the distribution of samples is Gaussian, implying that the noise is Gaussian as well (since the input signal is a constant value and does not have significant variation). As we move to the highest ND filter values, the distribution of recorded samples becomes more Poissonian (which we would expect in a shot-noise limited device such as a PMT), as shown in Figures 3 and 4 below:

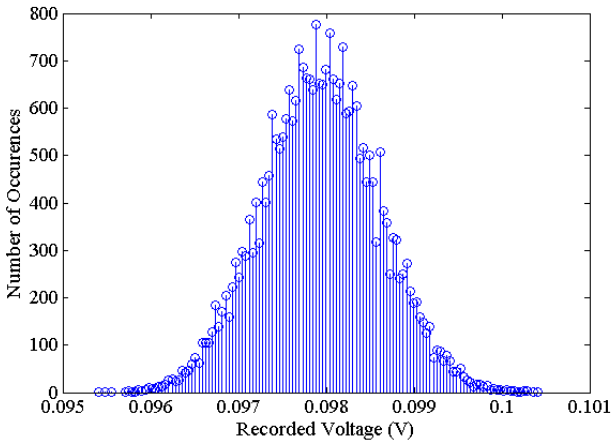

Figure 3: Histogram of captured samples, GV=503V, ND=5.0.

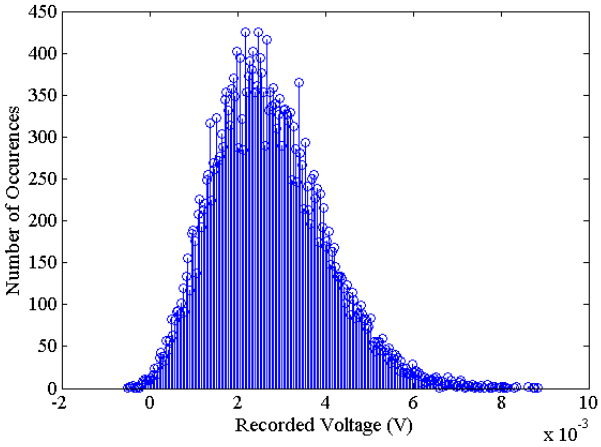

Figure 4: Histogram of captured samples, GV=876V, ND=8.7.

The SNR of the captured signals were calculated by taking the captured signal, taking the mean, and then taking the mean square difference between each sample and the mean. Then, the noise floor mean (as described above) was subtracted from the signal mean, and the noise floor variance was subtracted from the signal variance to get the corrected-mean and corrected-variance.

$$\mu_{corrected} = \mu_{signal} - \mu_{noisefloor} \tag{33}$$

$$\sigma^2 = \frac{\sum_t (V(t) - \mu_v)^2}{t} \tag{34}$$

$$\sigma^2_{corrected} = \sigma^2_{signal} - \sigma^2_{noisefloor} \tag{35}$$

$$SNR_{dB} = 10\log_{10}\left(\frac{\mu_{corrected}}{\sigma_{corrected}}\right) \tag{36}$$

Using the stochastic model, we start with an ideal signal where every sample is equal to the mean (86mW or 50mW depending on which experimental result we are comparing against). We attenuate the ideal signal by $10^{\text{ND-value}}$, convert from optical power to number of photons, reduce by the detector efficiency, then add noise to each sample according to equation (4). We convert this noisy signal to volts by multiplying by the terminal resistance (1 kΩ). Average SNR is again calculated using equations (33) and (34)

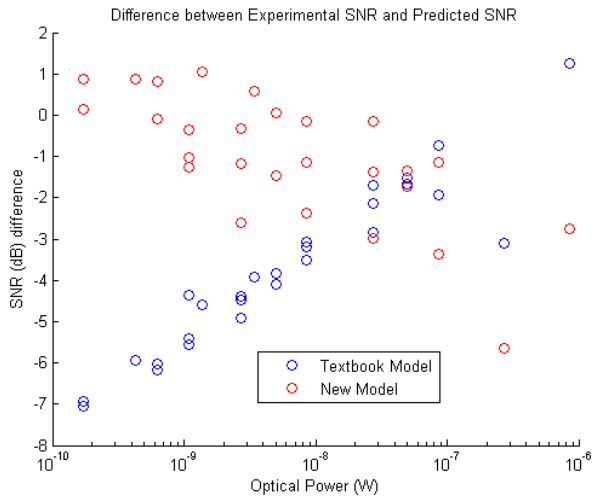

Figure 5: Optical power as calculated by the measured laser output and attenuated by the ND filter value.

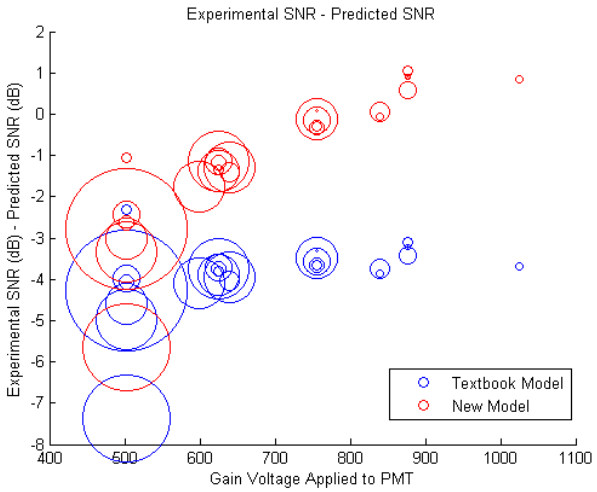

Figure 6: Bubble size indicates optical power (larger bubbles mean smaller ND filters used).

Figures 5 and 6 show the difference between the predicted average SNR and the observed SNR. An ideal noise model would have 0 difference between predicted and actual SNR. We can see that for the lowest optical power cases, the new model is much closer to the ideal (0 difference). The size of the circles in the bubble chart indicates the optical power entering the PMT. Note that the optical power (circle size) decreases as the gain voltage increases; This is done intentionally (with optical power being controlled by applying ND filters), to avoid damaging the PMT.

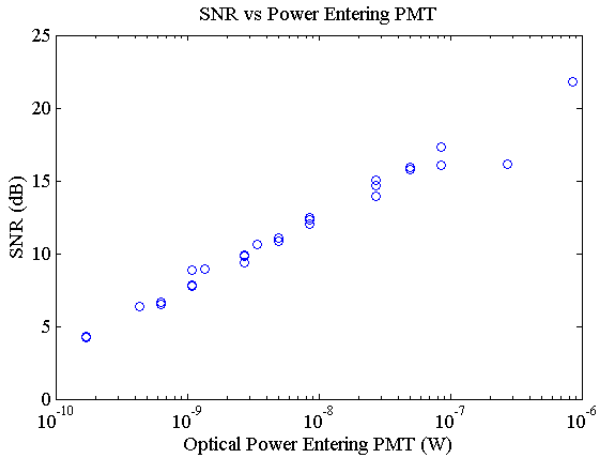

Figure 7: SNR vs optical power entering PMT as calculated by the measured laser output and attenuated by the ND filter value.

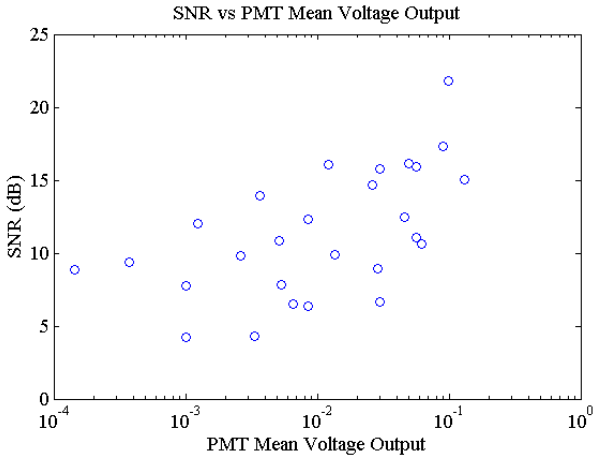

Figure 8: SNR vs PMT Voltage Output. Increased output voltage does not necessarily mean increased SNR.

We can also see that increased PMT voltage output does not necessarily correspond to increased SNR (Figure 8), while increasing the optical power entering the PMT does (Figure 7). This is consistent with a shot-noise-limited device, as increasing the gain will increase both the signal and the noise equally, having very little overall effect on the SNR.

VI. Conclusions and Future Work

The stochastic model provides very encouraging results, particularly in the case of low input power to the detector. The new model is more accurate in predicting the average SNR for low power cases than the standard textbook model, by as much as 7 dB in the lowest power case. However, more work is needed to allow us to apply noise directly to a simulated signal, as can be seen in Figures 9 and 10 below. Figure 10 in particular shows that our stochastic noise model produces noise that is more evenly distributed about the mean than is the case in the raw data output collected from the PMT as shown

in Figure 9. In future studies we will investigate what effect this discrepancy has on predicting bit error rates.

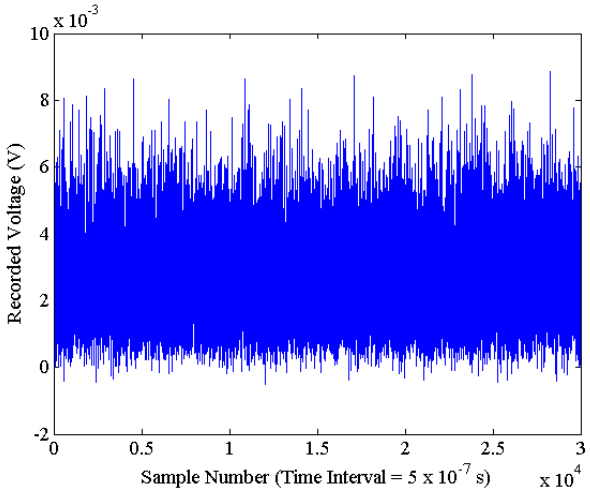

Figure 9: Raw data output collected from PMT for 876V Gain Voltage and 8.7 ND Filter. Low optical power as a result of the high ND filter results in a Poissonian noise distribution.

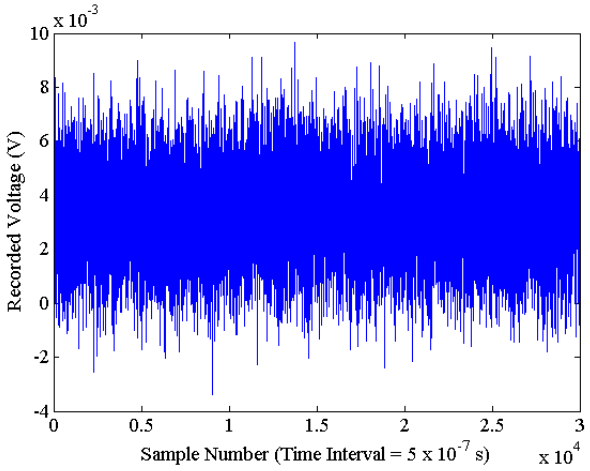

Figure 10: Simulated data output for 876V Gain Voltage and 8.7 ND Filter. Noise is more evenly distributed about the mean than in the PMT output data (shown in Figure 9)

Our next steps involve applying the noise model to actual at-sea laser-line-scan imaging data. Additionally, the non-stationary shot noise model will be applied to pulsed laser sources to investigate digital modulation techniques such as on-off-keying (OOK) and pulse-position-modulation (PPM).

VII. References

[1] Lacovara, P, "High-Bandwidth Underwater Communications", MARINE TECHNOLOGY SOCIETY JOURNAL, VOL. 42, NO. 1 (2008)

[2] Giddings, T. E., "Photomultiplier Receiver Model for Electro-Optical Systems", METRON TECH MEMO, 2008

[3] Boreman, G. D., "Basic Electro-Optics for Electrical Engineers", TUTORIAL TEXTS IN OPTICAL ENGINEERING, VOL. TT31 (1998)

[4] Palais, J. C., "Fiber Optic Communications", 5th Edition, PEARSON PRENTICE HALL (2005)

[5] van Etten, W. C., "Introduction to Random Signals and Noise", JOHN WILEY & SONS (2005).

[6] Ross, S. M., "A First Course in Probability", 7th Edition, PEARSON PRENTICE HALL (2006).

[7] Puri, P. S., "On the Characterization of Point Processes with the Order Statistic Property without the Moment Condition", J. APPL. PROB., VOL. 19, NO. 1, PP. 39-51, 1982.